FALDI-based decomposition of an atomic interaction line leads to 3D representation of the multicentre nature of interactions

Jurgens H. de Lange, Daniel M. E. van Niekerk and Ignacy Cukrowski

Correspondence to: Ignacy Cukrowski (E-mail: ignacy.cukrowski@up.ac.za)

Department of Chemistry, Faculty of Natural and Agricultural Sciences, University of Pretoria, Lynnwood Road, Hatfield, Pretoria 0002, South Africa

Electronic Supplementary Information

Table of Contents

Page No.:

PART 1. Coordinates of all the energy optimized structures investigated S2

PART 2. Additional FALDI decompositions of electron density (ED) computed for the diborane, *n*-butane, Schrock and Fischer carbene structures S5

PART 3. QTAIM properties at BCP(M,C) of Schrock and Fischer carbenes S7

PART 4. Discussion of FALDI-based 3D-isosurfaces of major *deloc*-ED of a bonding nature with respect to the M–C BCPs in the Schrock and Fischer carbene complex structures S8

PART 1

Coordinates of all the energy optimised structures investigated

Table S1. Cartesian coordinates of β-alanine.

Atom	X	Y	Z
C	1.088190	0.034622	0.025607
C	-0.015834	-0.990727	0.305358
H	0.364910	-1.963379	-0.007307
H	-0.147264	-1.035422	1.394001
O	0.695087	1.318470	-0.039570
H	-0.288824	1.362096	0.063494
O	2.242434	-0.281358	-0.103895
C	-1.366464	-0.701662	-0.362767
H	-1.226961	-0.605550	-1.442974
H	-2.043075	-1.548340	-0.196423
N	-1.919243	0.578448	0.129725
H	-2.679490	0.908449	-0.454885
H	-2.280115	0.482723	1.074548

Table S2. Cartesian coordinates of diborane.

Atom	X	Y	Z
B	0.000000	0.000000	0.883604
H	0.000000	1.037516	1.461235
H	0.000000	-1.037516	1.461235
B	0.000000	0.000000	-0.883605
H	0.000000	1.037516	-1.461235
H	0.000000	-1.037516	-1.461235
H	-0.976991	0.000000	0.000000
H	0.976991	0.000000	0.000000

Table S3. Cartesian coordinates of 'linear' *n*-butane.

Atom	**X**	**Y**	**Z**
H	-3.761122	2.225633	-0.931213
C	-3.702861	1.667088	0.008561
C	-3.389732	4.661081	2.528499
H	-3.331471	4.102536	3.468273
H	-3.087616	0.780435	-0.168238
H	-4.714439	1.327581	0.253589
H	-4.004977	5.547734	2.705298
H	-2.378154	5.000588	2.283472
C	-3.128229	2.537051	1.130022
H	-3.050947	1.946160	2.051204
H	-2.104335	2.837371	0.874949
C	-3.964363	3.791117	1.407039
H	-4.988258	3.490797	1.662112
H	-4.041646	4.382008	0.485857

Table S4. Cartesian coordinates of the Schrock carbene complex.

Atom	**X**	**Y**	**Z**
Ti	0.000000	0.298953	0.000000
C	1.823572	-0.722321	1.144494
C	1.582457	-1.518289	0.000001
C	2.246796	0.562186	0.709683
H	1.705489	-1.038273	2.171321
C	1.823572	-0.722322	-1.144494
H	1.235456	-2.539464	0.000001
C	2.246796	0.562185	-0.709684
H	2.512853	1.391790	1.344029
H	1.705489	-1.038275	-2.171320
H	2.512853	1.391788	-1.344031
C	-2.246797	0.562187	-0.709681
C	-1.823573	-0.722320	-1.144495
C	-2.246795	0.562184	0.709685
H	-2.512854	1.391791	-1.344026
C	-1.582457	-1.518289	-0.000002
H	-1.705492	-1.038271	-2.171322
C	-1.823571	-0.722324	1.144494
H	-2.512851	1.391787	1.344034
H	-1.235456	-2.539464	-0.000004
H	-1.705487	-1.038278	2.171320
C	0.000000	2.235441	0.000000
H	-0.892191	2.868997	0.000000
H	0.892191	2.868997	0.000000

Table S5. Cartesian coordinates of the Fischer carbene complex.

Atom	X	Y	Z
Cr	0.526063	-0.043880	0.000000
C	0.165674	-1.367682	1.341609
C	2.392338	-0.478539	0.000000
C	0.811865	1.276260	1.352450
C	0.811868	1.276262	-1.352447
C	0.165675	-1.367680	-1.341611
O	0.971439	2.074767	2.160486
O	3.509104	-0.737767	0.000000
O	-0.077475	-2.154682	2.136323
O	-0.077475	-2.154679	-2.136326
O	0.971444	2.074771	-2.160481
C	-1.445279	0.422140	0.000000
O	-2.331139	-0.559104	0.000000
C	-3.768105	-0.362274	-0.000001
H	-4.085364	0.174137	-0.895636
H	-4.187461	-1.365227	-0.000001
H	-4.085365	0.174137	0.895634
C	-2.034457	1.807614	-0.000001
H	-2.667948	1.960915	-0.882327
H	-2.667948	1.960916	0.882325
H	-1.256084	2.565204	-0.000001

End of PART 1

PART 2

Additional FALDI decompositions of electron density (ED) computed for the diborane, *n*-butane, Schrock and Fischer carbene structures

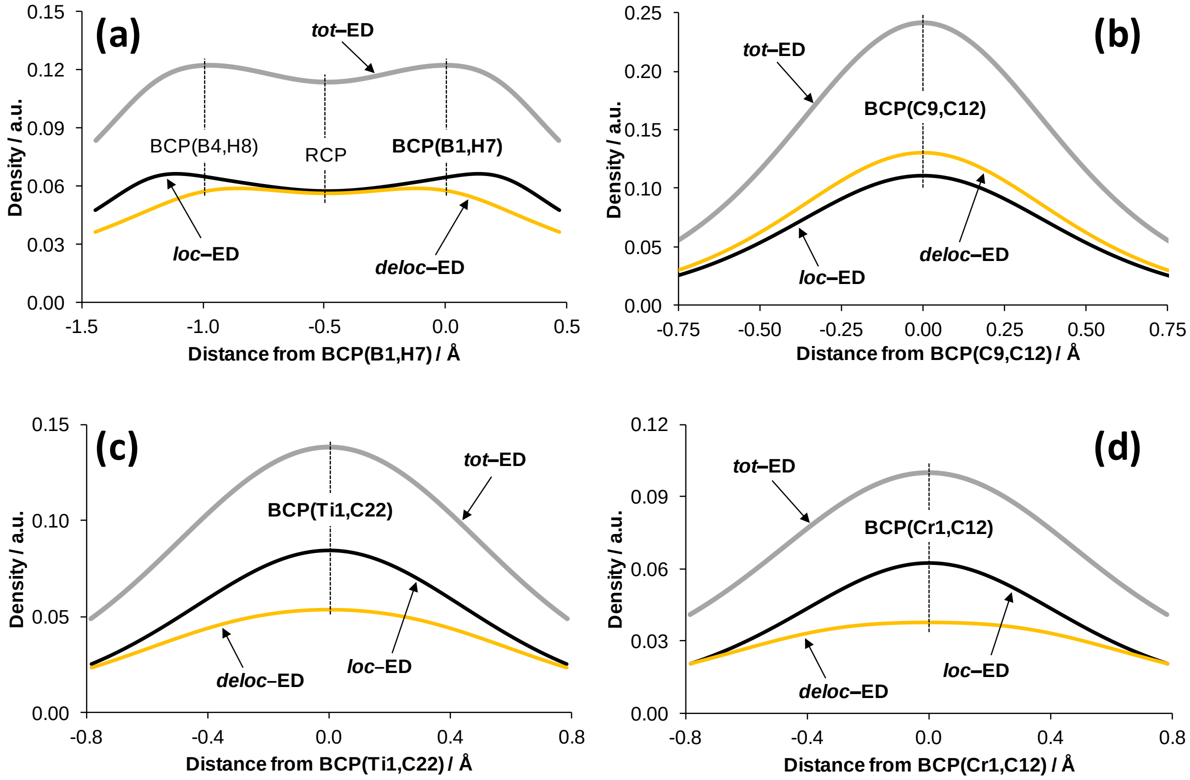

Figure S1. FALDI-based decompositions of the *tot*–ED (silver) in (**a**) diborane, (**b**) *n*-butane, (**c**) the Schrock carbene complex and (**d**) the Fischer carbene complex into *loc*– (black) and *deloc*–ED (gold) along the respective vectors indicated in Figure 1 (main text).

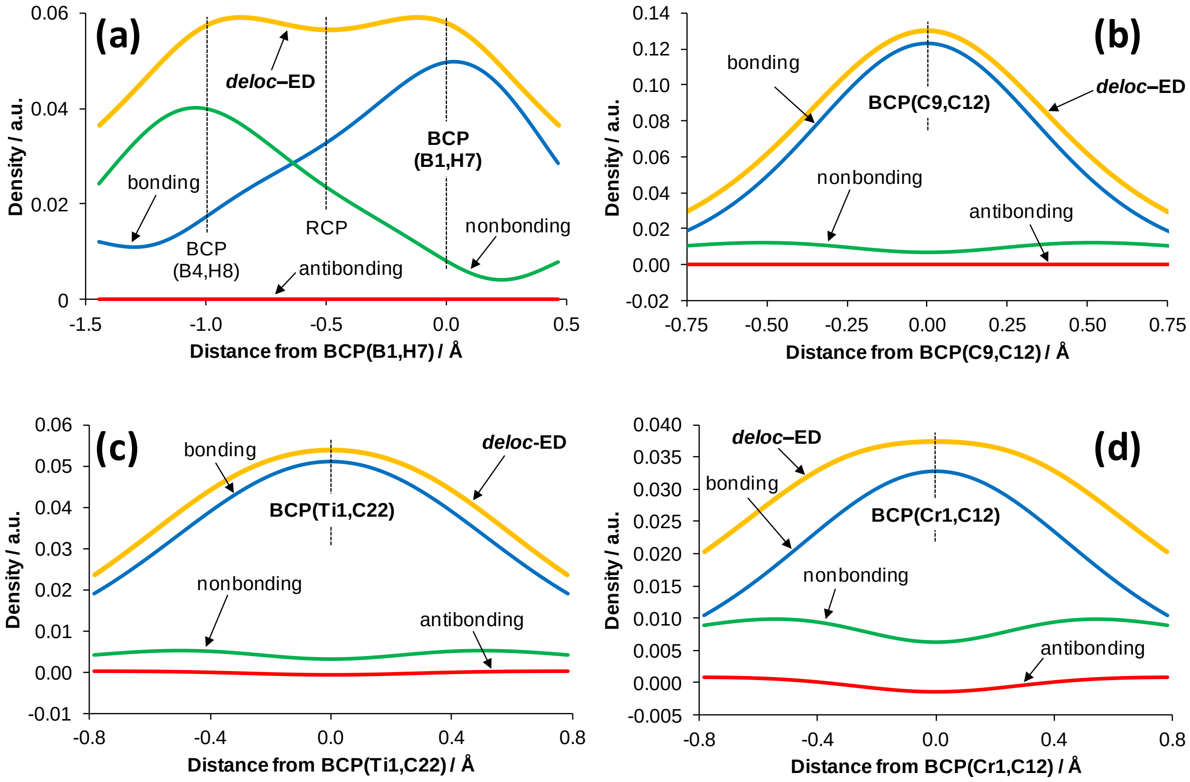

Figure S2. FALDI-based decompositions of the *deloc*–ED (gold) in (**a**) diborane, (**b**) *n*-butane, (**c**) the Schrock carbene complex and (**d**) the Fischer carbene complex into constructive (blue, bonding nature), nonconstructive (green, nonbonding nature) and deconstructive (red, antibonding nature) electron correlation with respect to the BCPs at which the multicentre bonding nature is explored, along the respective vectors indicated in Figure 1 (main text).

End of PART 2

PART 3

Table S6. QTAIM properties at BCP(M,C) of Schrock and Fischer carbenes.

	$\rho(\mathbf{BCP})^a$	$\nabla^2\rho(\mathbf{BCP})^a$	$\lvert V(\mathbf{BCP})\rvert/G(\mathbf{BCP})$	DI(M,C)
Schrock, $[(Cp)_2Ti=CH_2]$, **4**	0.1385	0.1731	1.61	1.37
Fischer, $[(CO)_5Cr=C(OCH_3)CH_3]$, **5**	0.0997	0.3062	1.28	0.76

a) In atomic units

End of PART 3

PART 4

Discussion of FALDI-based 3D-isosurfaces of major *deloc*-ED of a bonding nature with respect to the M–C BCPs in the Schrock and Fischer carbene complex structures

Figure S3 illustrates in real-space the 3D-isosurfaces of the three major contributing factors to the *deloc*–ED of a bonding nature with respect to the M–C BCPs in $[(Cp)_2Ti{=}CH_2]$ and $[(CO)_5Cr{=}C(OCH_3)CH_3]$ (corresponding to those summarised in pie-charts Figure 10, main text).

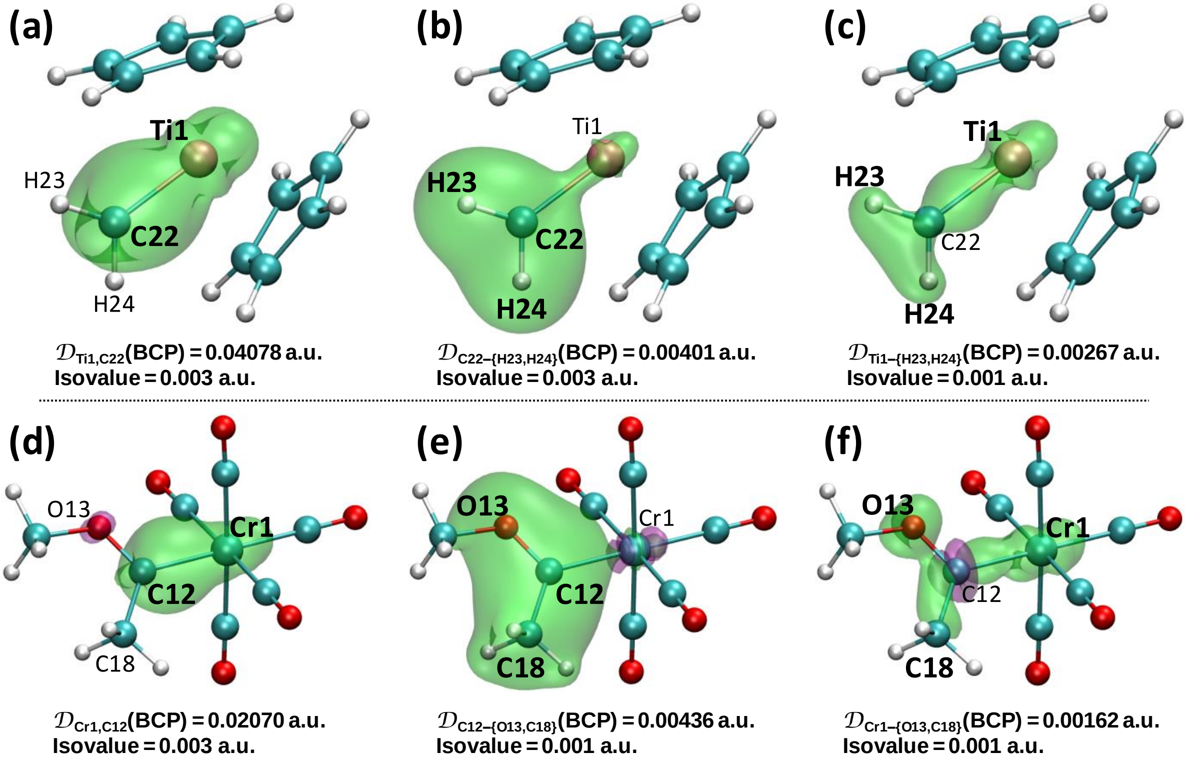

$\mathcal{D}_{Ti1,C22}$(BCP) = 0.04078 a.u.
Isovalue = 0.003 a.u.

$\mathcal{D}_{C22–\{H23,H24\}}$(BCP) = 0.00401 a.u.
Isovalue = 0.003 a.u.

$\mathcal{D}_{Ti1–\{H23,H24\}}$(BCP) = 0.00267 a.u.
Isovalue = 0.001 a.u.

$\mathcal{D}_{Cr1,C12}$(BCP) = 0.02070 a.u.
Isovalue = 0.003 a.u.

$\mathcal{D}_{C12–\{O13,C18\}}$(BCP) = 0.00436 a.u.
Isovalue = 0.001 a.u.

$\mathcal{D}_{Cr1–\{O13,C18\}}$(BCP) = 0.00162 a.u.
Isovalue = 0.001 a.u.

Figure S3. *Deloc*–ED 3D-isosurfaces of the major constructive electron correlation contributions made with respect to the M–C BCPs in the Schrock (**a**, **b** and **c**) and Fischer (**d**, **e** and **f**) carbene complexes: (**a**) $\mathcal{D}_{Ti1,C22}$ (80%), (**b**) $\mathcal{D}_{C22–\{H23,H24\}}$ (8%) and (**c**) $\mathcal{D}_{Ti1–\{H23,H24\}}$ (5%); (**d**) $\mathcal{D}_{Cr1,C12}$ (63%), (**e**) $\mathcal{D}_{C12–\{O13,C18\}}$ (13%) and (**f**) $\mathcal{D}_{Cr1–\{O13,C18\}}$ (5%). Colour coding: green = positive, purple = negative.

Considering the primary interaction's atom-pair, we note that the manner in which *deloc*–ED resulting from constructive electron correlation is distributed throughout the two carbene complex structures is quite similar, Figure S3 (**a** and **d**). In the case of $[(CO)_5Cr{=}C(OCH_3)CH_3]$, the primary interaction's atom-pair has a minor region of *deloc*–ED resulting from deconstructive electron correlation at heteroatom O13. Other than that, the general shape and size of the constructive electron correlation isosurfaces in both complexes are essentially the same, with a concentration in their respective interatomic regions, specifically at the M–C BCPs. Furthermore, it is very illuminating to visualise how the *deloc*–ED (of a bonding nature) within each ligand, such as that of atom-pair combination C22 with {H23,H24} in (**4**) and C12 with {O13,C18} in (**5**), extends and facilitates the formation of the M–C BCPs, Figure S3 (**b** and **e**). We also note in $[(CO)_5Cr{=}C(OCH_3)CH_3]$ the manner in which electrons are delocalized between Cr1 and {O13,C18} occurs through the M–C bond rather than directly through space, Figure S3 (**f**). In these instances, the M–C bond acts as a bridge for long distance electron correlation effects. Although both the *non*-heteroatom H23 (or H24) in $[(Cp)_2Ti{=}CH_2]$ and heteroatom O13 in $[(CO)_5Cr{=}C(OCH_3)CH_3]$ concentrate ED at their respective M–C BCPs, the contribution by O13 is percentage-wise considerably larger in magnitude, Figure 10 (main text).

End of PART 4